Proceedings of the 3rd International Conference on
Systems and Control, Algiers, Algeria,
October 29-31, 2013

freepapers.ir FREE papers

Robust Trajectory Tracking Control of a Quadrotor UAV

Karima Benzaid[1] and Noura Mansouri[1] and Ouiddad Labbani-Igbida[2]

Abstract— **In this paper, we present two control strategies of a quadrotor Unmanned Aerial Vehicle (UAV). The dynamics of the system is controlled to achieve a complex trajectory tracking. A controller using the integral backstepping is developed for the stabilization of the six degrees of freedom (6DoF) of the system. Furthermore, we propose a hybrid strategy by combining the integral backstepping and the PID linear controller. For this, we divide the dynamic system into two subsystems; each one with 3DoF. For the stabilization of the rotational dynamics, the PID controller is proposed. The Integral Backstepping is applied for the longitudinal, lateral and vertical position stabilization. Finally, some numerical simulations are conducted to illustrate the robustness of both strategies.**

I. Introduction

Research related to UAVs has been extensively developed in the recent decades, thanks to the technological advances in the field of actuators miniaturization and onboard electronics. A quadrotor is an UAV which has known a great development in the field of control. In [1], a flight control based on Lyapunov analyses using a nested saturation algorithm was designed and implemented on a mini quadrotor. The dynamic model was obtained via Lagrange approach. The proposed controller performance was tested in real-time experiments performing indoors, the tasks of taking off, hovering and landing. A variant of this strategy was developed in [2] using the optical flow measurements, and tested in a real-time experiment to achieve an eight-rotor rotorcraft hover flight. An optical flow-based terrain following algorithm for mini rotorcraft was proposed in [3]. The authors in [4] proposed a nonlinear control algorithm using sliding mode for the control of the vertical position and the rotational displacement of a quadrotor in presence of external disturbance and actuator fault. The controller was validated in simulation. The same algorithm was studied in [5] to design a controller applied to a 4Y octorotor. This UAV configuration is an extension of the popular quadrotor by adding four more rotors. Numerical simulations were given in order to test the efficiency of the approach. The problem of the longitudinal and lateral position stabilization of an autonomous helicopter in a hover flight was considered in [6]. Two controllers were proposed in this concept: the first one is based on the backstepping algorithm, and the second, on a linear quadratic regulator criteria (LQR). The comparison between the two control algorithms in presence of wind was carried out using simulation. Different variants of the recursive algorithm backstepping were developed for the control of a 3DoF helicopter (consists of two motors and a counterweight acting as a counterbalance) in [7] and, a miniature autonomous helicopter with constant inertial parameter uncertainties in [8]. The work proposed in [9] presents an analysis of various extensions of the backstepping algorithm, more specifically, including the integral action. Other linear, nonlinear or intelligent control techniques have been cited in [10].

In this paper, we are interested in the control of a quadrotor unmanned aerial vehicle with the objective of stabilizing the system on a desired trajectory. The reference trajectory is of 6DoF and chosen to be complex (half circle, corner and helical). To achieve this purpose, we propose two approaches: the first one is based on the integral backstepping algorithm for the control of the full dynamics of the system; the second is a new hybrid strategy which combines a PID controller and an integral backstepping. The PID is used to ensure the rotational subsystem stabilization and, the integral backstepping is applied to ensure the translational dynamics stability. The advantage of this hybrid strategy is to combine the performance of both controllers for trajectory tracking.

This paper is organized as follows. Section II introduces the quadrotor dynamic model. The identification of the quadrotor inputs/outputs and the modeling for control are given in Section III. Section IV presents the design of the proposed strategies and the analysis by Lyapunov theory. Numerical simulation results using Matlab/Simulink environment are shown in Section V before concluding in Section VI.

II. Quadrotor Dynamics

Considering the quadrotor configuration, four identical rotors and propellers are equipped on each end of a rigid square platform (see Fig. 1).

The motor M_i (for $i = 1 : 4$) produces the force f_i, which is proportional to the square of the angular speed, that is, $f_i = b\ \omega_i^2$ with b is the thrust coefficient. Given the quadrotor configuration (Fig. 1) and assuming that the two motors aligned with x-axis rotate clockwise while the other two motors rotate counter-clockwise, the resulting force vector F is the sum of the thrusts of the individual motors. The roll movement is obtained by increasing (resp. reducing) the speed of the second motor while reducing (resp. increasing) the speed of the fourth motor. The pitch movement is obtained similarly using the other motors. The yaw movement is obtained by increasing (resp. decreasing) the speed of the second and fourth motors while decreasing

[1]K. Benzaid and N. Mansouri are with Laboratory of Automatic Control and Robotics, Constantine1 University, Constantine, 25000 Algeria kari_benzaid@yahoo.fr, nor_mansouri@yahoo.fr

[2]O. Labbani-Igbida is with Modeling, Information & Systems lab., University of Picardie Jules Verne, Amiens, France ouiddad.labbani@u-picardie.fr

978-1-4799-0275-0/13/$31.00 ©2013 IEEE

دانلود کننده مقالات علمی freepapers.ir FREE papers

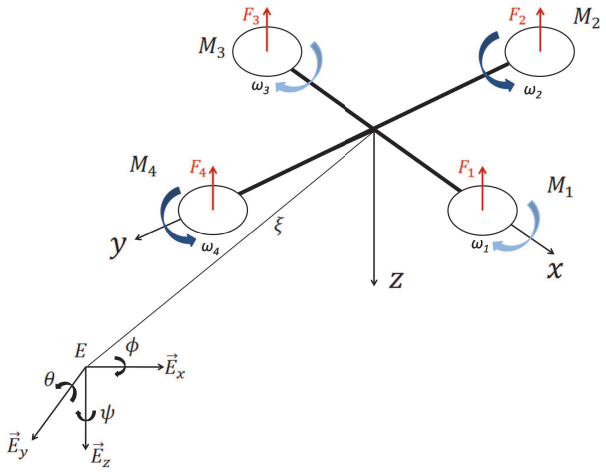

Fig. 1: Quadrotor model in the inertial frame $E = \{\vec{E}_x, \vec{E}_y, \vec{E}_z\}$.

(resp. increasing) the speed of the first and third motors [11]. This leads to:

$$\begin{cases} F = \sum_{i=1}^{4} F_i = b \sum_{i=1}^{4} \omega_i^2 \\ \Gamma_r = l(F_2 - F_4) = bl(\omega_2^2 - \omega_4^2) \\ \Gamma_p = l(F_1 - F_3) = bl(\omega_1^2 - \omega_3^2) \\ \Gamma_y = d(-\omega_1^2 + \omega_2^2 - \omega_3^2 + \omega_4^2) \end{cases} \quad (1)$$

where Γ_r, Γ_p and Γ_y are the roll, pitch and yaw torques. l is the distance from the center of the mass to the center of each rotor in the plane (x, y) and d is the drug coefficient.

Let $\xi = [x\ y\ z]^t$ denote the position vector of the center of mass of the quadrotor relative to a fixed inertial frame $E = \{\vec{E}_x, \vec{E}_y, \vec{E}_z\}$ with $\vec{E}_z$ the vertical axis directed downwards, and $\eta = [\phi\ \theta\ \psi]^t$ denotes the Euler angles with ϕ the roll angle around the x-axis, θ the pitch angle around y-axis and ψ the yaw angle around z-axis.

Two formalisms are used to obtain state equations describing the quadrotor dynamics: Euler-Newton formalism and Euler-Lagrange formalism. Using the latter, the dynamic model of the quadrotor can be written [12] as follows:

$$\begin{cases} \ddot{x} = -\frac{1}{m}(\cos\phi \sin\theta \cos\psi + \sin\phi \sin\psi).F \\ \ddot{y} = -\frac{1}{m}(\cos\phi \sin\theta \sin\psi - \sin\phi \cos\psi).F \\ \ddot{z} = g - \frac{\cos\phi \cos\theta}{m}.F \\ \ddot{\phi} = \frac{(I_{yy} - I_{zz})}{I_{xx}}\dot{\theta}\dot{\psi} + \frac{I_r}{I_{xx}}\omega_g\dot{\theta} + \frac{\Gamma_r}{I_{xx}} \\ \ddot{\theta} = \frac{(I_{zz} - I_{xx})}{I_{yy}}\dot{\phi}\dot{\psi} - \frac{I_r}{I_{yy}}\omega_g\dot{\phi} + \frac{\Gamma_p}{I_{yy}} \\ \ddot{\psi} = \frac{(I_{xx} - I_{yy})}{I_{zz}}\dot{\phi}\dot{\theta} + \frac{\Gamma_y}{I_{zz}} \end{cases} \quad (2)$$

where:

$$\omega_g = \omega_1 - \omega_2 + \omega_3 - \omega_4$$

with m is the total mass of the quadrotor, g the gravitational acceleration. I_{xx}, I_{yy} and I_{zz} are the inertia moments and I_r the rotors inertia.

III. Modelling For Control

The identification of the system inputs/outputs is the first step of the control strategy design. A miniature rotorcraft in displacement in the 3D space, is located by its longitudinal, lateral and vertical position. Its orientation is determined by the roll, pitch and yaw angles. So, it has 6DoF. Considering the particular case of a quadrotor, the motors rotation speeds are to be controlled indirectly by controlling the resultant thrust force F, and the roll, pitch and yaw torques. Thus, the quadrotor is an under-actuated system with six outputs and four inputs. $U = [U_1\ U_2\ U_3\ U_4]^t$ is the inputs vector chosen as follows:

$$\begin{cases} U_1 = b(\omega_1^2 + \omega_2^2 + \omega_3^2 + \omega_4^2) \\ U_2 = b(\omega_2^2 - \omega_4^2) \\ U_3 = b(\omega_1^2 - \omega_3^2) \\ U_4 = d(-\omega_1^2 + \omega_2^2 - \omega_3^2 + \omega_4^2) \end{cases} \quad (3)$$

From equations (2) and (3), we obtain:

$$\begin{cases} \ddot{x} = -\frac{1}{m}u_x U_1 \\ \ddot{y} = -\frac{1}{m}u_y U_1 \\ \ddot{z} = g - \frac{\cos\phi \cos\theta}{m}U_1 \\ \ddot{\phi} = \frac{(I_{yy} - I_{zz})}{I_{xx}}\dot{\theta}\dot{\psi} + \frac{I_r}{I_{xx}}\omega_g\dot{\theta} + \frac{l}{I_{xx}}U_2 \\ \ddot{\theta} = \frac{(I_{zz} - I_{xx})}{I_{yy}}\dot{\phi}\dot{\psi} - \frac{I_r}{I_{yy}}\omega_g\dot{\phi} + \frac{l}{I_{yy}}U_3 \\ \ddot{\psi} = \frac{(I_{xx} - I_{yy})}{I_{zz}}\dot{\phi}\dot{\theta} + \frac{1}{I_{zz}}U_4 \end{cases} \quad (4)$$

where:

$$u_x = \cos\phi \sin\theta \cos\psi + \sin\phi \sin\psi \quad (5)$$

$$u_y = \cos\phi \sin\theta \sin\psi - \sin\phi \cos\psi \quad (6)$$

IV. Control Strategies

The global scheme of flight control is depicted in Fig. 2. We develop in this section two control strategies based respectively on the integral backstepping and a new hybrid approach for trajectory following.

A. Control using integral backstepping

The backstepping controller is based on a recursive algorithm. It is used to control linear and nonlinear under-actuated systems. The aim of adding the integral action is to improve the efficiency of the basic approach.

We have divided the system structure into six sub-systems describing the 6DoF. The key idea of backstepping is to design a virtual controller for each sub-system by associating a Lyapunov function. And then, step back the feedback signal towards the real control input by considering an extended Lyapunov function [13][14][15].

978-1-4799-0275-0/13/$31.00 ©2013 IEEE

freepapers.ir FREE papers دانلود کننده مقالات علمی

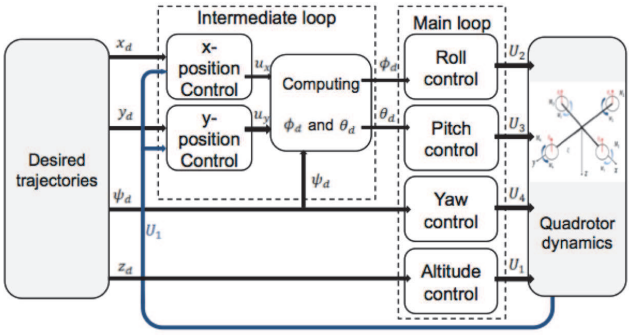

Fig. 2: Global structure of a quadrotor strategy control.

1) Altitude control: Figure (3) illustrates the integral backstepping approach applied to control the vertical position.

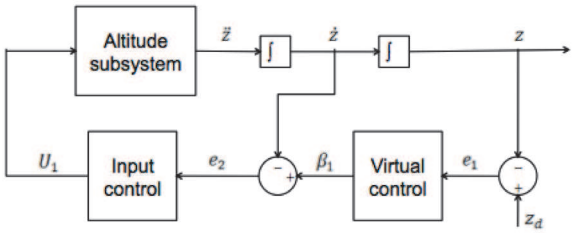

Fig. 3: Backstepping approach design.

The trajectory tracking error of the z-position is given by e_1:

$$e_1 = z_d - z, \quad \dot{e}_1 = \dot{z}_d - \dot{z}$$

Including the integral action, the positive definite Lyapunov function $V(e_1)$ is chosen as follows:

$$V(e_1) = \frac{1}{2}\left[e_1^2 + \lambda_1 \left(\int_0^t e_1(\tau)d\tau\right)^2\right], \lambda_1 > 0$$

Its time derivative is:

$$\dot{V}(e_1) = e_1\left(\dot{z}_d - \dot{z} + \lambda_1 \int_0^t e_1(\tau)d\tau\right) \tag{7}$$

To have $\dot{V}(e_1)$ negative semi-definite, we consider $\dot{z}$ as a virtual control input, in which we impose a desired behavior β_1.

$$\beta_1 = \dot{z}_d + \lambda_1 \int_0^t e_1(\tau)d\tau + c_1 e_1, c_1 > 0$$

Substituting $\dot{z}$ in (7) by β_1, we obtain:

$$\dot{V}(e_1) = -c_1 e_1^2 \leq 0$$

Going back to the previous step, $\dot{z}$ does not necessarily converge to the desired behavior β_1. We must correct e_2 error defined as follows:

$$e_2 = \beta_1 - \dot{z} = \dot{z}_d + \lambda_1 \int_0^t e_1(\tau)d\tau + c_1 e_1 - \dot{z} \tag{8}$$

then, its time derivative is:

$$\dot{e}_2 = \ddot{z}_d + \lambda_1 e_1 + c_1 \dot{e}_1 - \ddot{z}$$

The extended Lyapunov function is given in (9) to stabilize e_1 and e_2 errors.

$$V(e_1, e_2) = \frac{1}{2}\left[e_1^2 + e_2^2 + \lambda_1 \left(\int_0^t e_1(\tau)d\tau\right)^2\right] \tag{9}$$

Indeed, its time derivative is:

$$\dot{V}(e_1, e_2) = e_1\left(\dot{e}_1 + \lambda_1 \int_0^t e_1(\tau)d\tau\right) + e_2\dot{e}_2 \tag{10}$$

From (8), we can write:

$$\dot{e}_1 = \dot{z}_d - \dot{z} = e_2 - \lambda_1 \int_0^t e_1(\tau)d\tau - c_1 e_1$$

Substituting $\dot{e}_1$ and $\dot{e}_2$ in (10), we obtain:

$$\begin{aligned}\dot{V}(e_1, e_2) = -c_1 e_1^2 + e_2 \big[&(1 - c_1^2 + \lambda_1)e_1 + c_1 e_2 + \ddot{z}_d \\ &- c_1\lambda_1 \textstyle\int_0^t e_1(\tau)d\tau - \ddot{z}\big]\end{aligned} \tag{11}$$

Note that $\ddot{z}$ is function of U_1 input (4). That is why U_1 must be chosen such that $\dot{V}(e_1, e_2)$ is negative semi-definite. If we take:

$$\begin{aligned}U_1 = a\big[&g - \ddot{z}_d - (1 - c_1^2 + \lambda_1)e_1 - (c_1 + c_2)e_2 \\ &+ c_1\lambda_1 \textstyle\int_0^t e_1(\tau)d\tau\big]\end{aligned} \tag{12}$$

with $a = \dfrac{m}{\cos\phi\cos\theta}$ and $c_2 > 0$, then $\dot{V}(e_1, e_2) = -c_1 e_1^2 - c_2 e_2^2 \leq 0$.

2) Lateral and longitudinal position control: The translational dynamics in x (resp. y) direction is a function of U_1, and u_x (resp. u_y) control inputs. Following the same steps as the altitude control, we can write:

$$\begin{cases} e_3 = x_d - x \\ e_4 = \dot{x}_d + \lambda_2 \int_0^t e_3(\tau)d\tau + c_3 e_3 - \dot{x} \end{cases}$$

To guarantee the convergence of e_3 and e_4 to zero, u_x is chosen as follows:

$$\begin{aligned}u_x = \tfrac{m}{U_1}\big[&-\ddot{x}_d - (1 - c_3^2 + \lambda_2)e_3 - (c_3 + c_4)e_4 \\ &+ c_3\lambda_2 \textstyle\int_0^t e_3(\tau)d\tau\big]\end{aligned} \tag{13}$$

with $c_3, c_4, \lambda_2 > 0$.

Similarly, we define:

$$\begin{cases} e_5 = y_d - y \\ e_6 = \dot{y}_d + \lambda_3 \int_0^t e_5(\tau)d\tau + c_5 e_5 - \dot{y} \end{cases}$$

We choose the u_y control input as follows:

$$\begin{aligned}u_y = \tfrac{m}{U_1}\big[&-\ddot{y}_d - (1 - c_5^2 + \lambda_3)e_5 - (c_5 + c_6)e_6 \\ &+ c_5\lambda_3 \textstyle\int_0^t e_5(\tau)d\tau\big]\end{aligned} \tag{14}$$

with $c_5, c_6, \lambda_3 > 0$.

978-1-4799-0275-0/13/$31.00 ©2013 IEEE

freepapers.ir FREE papers

3) Yaw Control: We consider the yaw trajectory tracking error e_7 and the tracking error e_8 of the virtual control $\dot{\psi}$ with a desired behavior α_1.

$$\begin{cases} e_7 = \psi_d - \psi \\ e_8 = \alpha_1 - \dot{\psi} = \dot{\psi}_d + \lambda_4 \int_0^t e_7(\tau)d\tau + c_7 e_7 - \dot{\psi} \end{cases}$$

The extended Lyapunov function is given by:

$$V(e_7, e_8) = \frac{1}{2}\left[e_7^2 + e_8^2 + \lambda_4 (\int_0^t e_7(\tau)d\tau)^2\right]$$

and its time derivative is:

$$\dot{V}(e_7, e_8) = -c_7 e_7^2 + e_8\left[(1 - c_7^2 + \lambda_4)e_7 + c_7 e_8 + \ddot{\psi}_d - c_7\lambda_4 \int_0^t e_7(\tau)d\tau - \frac{I_{xx}-I_{yy}}{I_{zz}}\dot{\phi}\dot{\theta} - \frac{1}{I_{zz}}U_4\right]$$

U_4 is the input control for the yaw angle. It should be chosen such that the Lyapunov function derivative is negative semi-definite. If one chooses:

$$U_4 = I_{zz}\left[-\frac{(I_{xx}-I_{yy})}{I_{zz}}\dot{\phi}\dot{\theta} + \ddot{\psi}_d + (1 - c_7^2 + \lambda_4)e_7 + (c_7 + c_8)e_8 - c_7\lambda_4 \int_0^t e_7(\tau)d\tau\right] \quad (15)$$

with $c_7, c_8, \lambda_4 > 0$, then $\dot{V}(e_7, e_8) = -c_7 e_7^2 - c_8 e_8^2 \leq 0$.

4) Roll and pitch control: The roll desired trajectory is constrained by equations (5) and (6) while the yaw desired trajectory is set by the operator. Note also that the u_x and u_y control inputs are given by (13) and (14) to achieve the desired x, y-trajectory. So, we can write:

$$\phi_d = \arcsin(u_x . \sin\psi_d - u_y . \cos\psi_d) \quad (16)$$

After obtaining ϕ_d, the pitch desired trajectory can be calculated as follows:

$$\theta_d = \arcsin\left(\frac{u_x . \cos\psi_d + u_y . \sin\psi_d}{\cos\psi_d}\right) \quad (17)$$

Using the same integral backstepping approach, the U_2 and U_3 control inputs can be written as:

$$U_2 = \frac{I_{xx}}{l}\left[-\frac{(I_{yy}-I_{zz})}{I_{xx}}\dot{\theta}\dot{\psi} - \frac{I_r}{I_{xx}}\omega_g\dot{\theta} + \ddot{\phi}_d + (c_9 + c_{10})e_{10} + (1 - c_9^2 + \lambda_5)e_9 - c_9\lambda_5 \int_0^t e_9(\tau)d\tau\right] \quad (18)$$

and

$$U_3 = \frac{I_{yy}}{l}\left[-\frac{(I_{zz}-I_{xx})}{I_{yy}}\dot{\phi}\dot{\psi} + \frac{I_r}{I_{yy}}\omega_g\dot{\phi} + \ddot{\theta}_d + (c_{11} + c_{12})e_{12} + (1 - c_{11}^2 + \lambda_6)e_{11} - c_{11}\lambda_6 \int_0^t e_{11}(\tau)d\tau\right] \quad (19)$$

with $c_9, c_{10}, c_{11}, c_{12}, \lambda_5, \lambda_6 > 0$.

B. Hybrid control strategy

The hybrid proposed strategy is applied to stabilize the quadrotor by dividing the dynamic model into two subsystems, each one is of 3DoF. This strategy is built in a hierarchical two-loop architecture. The inner loop controls the attitude using a PID controller. While, the outer loop controls the 3D translational dynamics using integral backstepping (see Fig. 4). The PID controller is one of the most successful linear controllers. Thanks to its simplicity and robustness, it was implemented and it is still used in most flight robotic projects. This hybrid approach allows us to combine the integral backstepping and PID advantages.

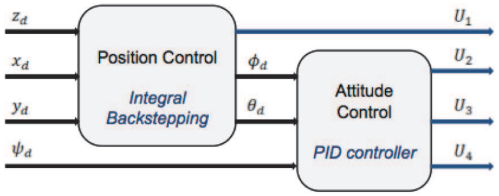

Fig. 4: The proposed hybrid control strategy.

The design of the outer loop to achieve the stability of the (x, y, z)-position is identical to the one developed in the previous section.

The control input of the PID controller is defined by:

$$U = K_P e(t) + K_I \int_0^t e(\tau)d\tau + K_D \frac{de(t)}{dt}$$

where e is the tracking error.

The design of a PID controller needs a good choice of the parameters K_P, K_I and K_D which represent the proportional, integral and derivative gains. The control inputs of the attitude dynamics obtained by applying the PID controller are:

$$\begin{cases} U_2 = K_{P\phi} e_\phi(t) + K_{I\phi} \int_0^t e_\phi(\tau)d\tau + K_{D\phi} \frac{de_\phi(t)}{dt} \\ U_3 = K_{P\theta} e_\theta(t) + K_{I\theta} \int_0^t e_\theta(\tau)d\tau + K_{D\theta} \frac{de_\theta(t)}{dt} \\ U_4 = K_{P\psi} e_\psi(t) + K_{I\psi} \int_0^t e_\psi(\tau)d\tau + K_{D\psi} \frac{de_\psi(t)}{dt} \end{cases} \quad (20)$$

A comparative study between the two strategies discussing the robustness, simplicity and convergence time is given in Section V to prove the performance of the proposed strategies.

V. Results And Discussions

The two strategies inputs control designed in the previous sections are implemented under Matlab/Simulink environment with the physical parameters [12]: $m = 0.65$ kg, $I_{xx} = I_{yy} = 7.5\ 10^{-3}$ kgm^2, $I_{zz} = 1.3\ 10^{-2}$ kgm^2, $I_r = 3.13\ 10^{-5}$ kgm^2, $b = 3.13\ 10^{-5}$ Ns^2, $d = 7.510^{-7}$ Nms^2, $l = 0.23$ m and $g = 9.81$ m/s^2. The integral backstepping and PID controller gains are obtained using the Optimization Toolbox under Matlab. $c_1 = 3.52, c_2 = 2, \lambda_1 = 6.93\ 10^{-18}, c_3 = 9.99, c_4 = 2.24, \lambda_2 = 4.43\ 10^{-4}, c_5 = 9.99, c_6 = 1.99, \lambda_3 = 3.99\ 10^{-4}, c_7 = 2, c_8 = 2, \lambda_4 = 10^{-4}, c_9 = 10, c_{10} = 2, \lambda_5 = 10^{-4}, c_{11} = 10, c_{12} = 2, \lambda_6 = 10^{-4}, K_{P\phi} = 0.8, K_{I\phi} = 0, K_{D\phi} = 0.4, K_{P\theta} = 0.8, K_{I\theta} = 0, K_{D\theta} = 0.4, K_{P\psi} = 0.8, K_{I\psi} = 0, K_{D\psi} = 0.5$.

The controller aims to realize trajectory tracking by controlling the 6DoF of the quadrotor. The reference trajectory contains coins, half circles and helicals to test the effectiveness of the developed strategies. The initial conditions are taken $(0.5, 0.5, 0.3)$ m for the (x, y, z)-position vector and

978-1-4799-0275-0/13/$31.00 ©2013 IEEE

freepapers.ir FREE papers

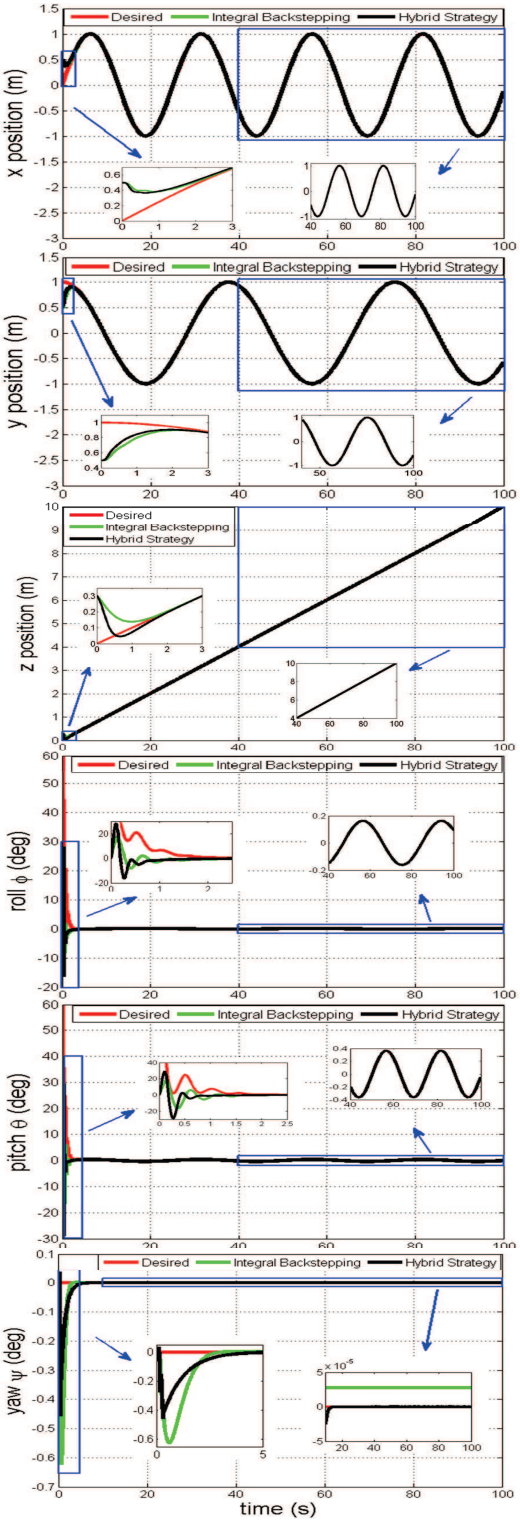

Fig. 5: Trajectory tracking results of the quadrotor *(from the top down)* (x, y, z)-position (m) and (ϕ, θ, ψ)-attitude (deg) vs. time (s), using integral backstepping control (in *green*) and hybrid control (in *black*) strategies. Local zooms are shown for the transient and the steady state responses.

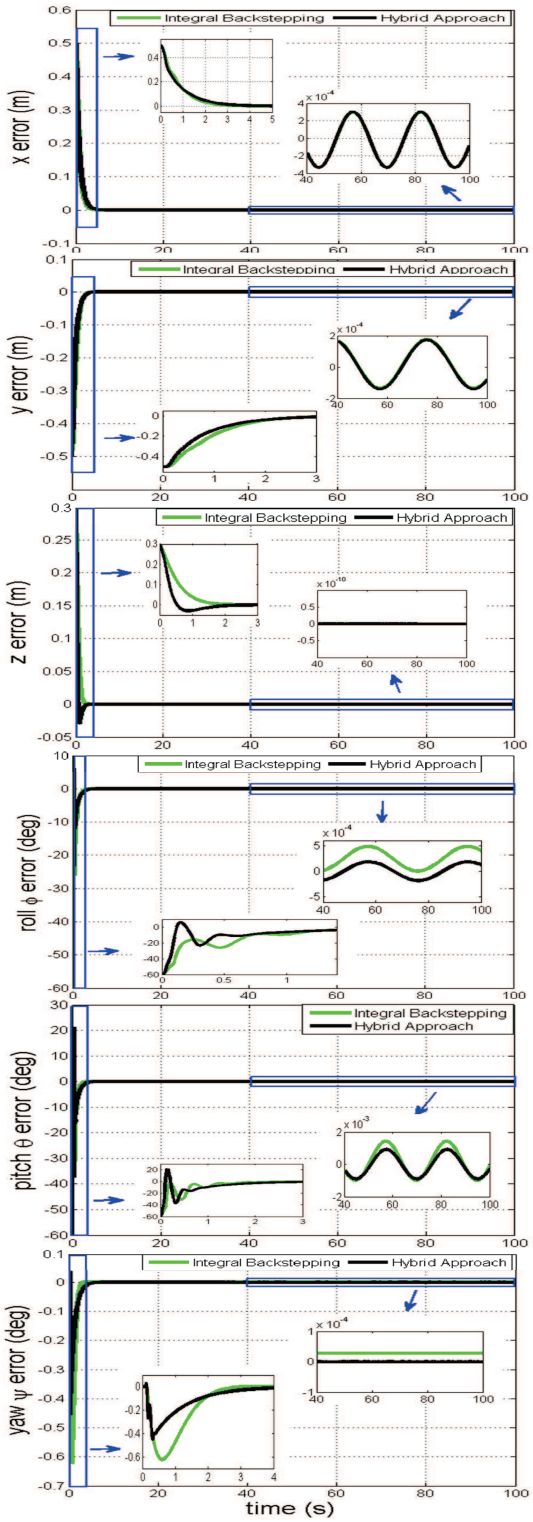

Fig. 6: Trajectory tracking error of *(from the top down)* the (x, y, z)-position (m) and (ϕ, θ, ψ)-attitude (deg) of the quadrotor vs. time (s), using integral backstepping control (in *green*) and hybrid control (in *black*) strategies. Local zooms are shown for the transient and the steady state responses.

978-1-4799-0275-0/13/$31.00 ©2013 IEEE

freepapers.ir FREE papers دانلود کننده مقالات علمی

$\psi = 0$ for the yaw angle. The referential trajectories for the roll and pitch angles are calculated to achieve the desired longitudinal and lateral trajectories. In other words, the latter trajectories determine the necessary quadrotor inclination to reach the desired point in (x, y)-plane (equations (16) and (17)). From the numerical results, we can see that the roll and pitch angles follow a sinusoidal movement which is the same form of the (x, y)-desired trajectories.

The trajectory tracking results of the proposed control strategies are shown in Fig. 5. In the transient response, the controllers show different behaviors. After five seconds, the response becomes stable. In the steady response, the trajectories of the both proposed strategies conform to the desired trajectory. A comparative study is carried out by plotting the trajectory tracking error of the six variables with a zoom on the transient and steady state responses (Fig. 6). The z-position stabilization error is equal to zero while the x, y-position stabilization errors are in the order of 10^{-4}. Discussing the attitude control error, the roll and pitch-angle errors are closer to zero using the PID controller (hybrid strategy) compared with the integral backstepping. The yaw angle error is equal to zero for the hybrid strategy but is in the order of 10^{-4} for the integral backstepping strategy. According to these results, the new strategy demonstrates its robustness and presents more aptitude to realize the quadrotor 6DoF trajectory tracking despite its simplicity. Figure 7 shows the 3D desired trajectory and, those obtained using both strategies with a zoom on the starting trajectories.

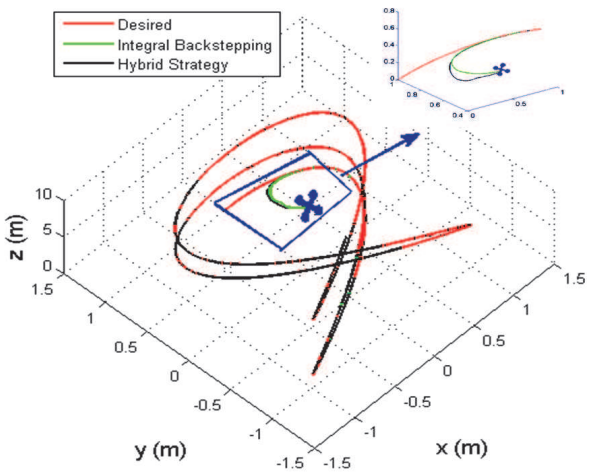

Fig. 7: 3D trajectory of the quadrotor obtained by (in *green*) integral backstepping control and (in *black*) hybrid control. The desired trajectory is shown in *red* with a zoom *(top right)* on the start trajectories.

VI. Conclusion

In this paper, two robust and efficient control strategies are developed and implemented under Matlab to ensure complex trajectory following of a quadrotor UAV. The first strategy, the integral backstepping, is applied to control the 6DoF of the quadrotor and the numerical results showed its efficiency. The second one is a new strategy proposed by combining the integral backstepping and a PID controller. As done in the first strategy, the use of the integral backstepping (outer loop) stabilized the (x, y, z)-position. The PID algorithm controls the attitude of the system and gave good results by canceling the tracking error. The latter strategy proved a high performance for the quadrotor 6DoF control where the 3D reference trajectory is perfectly achieved. The choice of a control strategy to be implemented on a real time platform is a compromise between the simplicity, the robustness and the rapidity for data up to date in real time. The hybrid strategy takes advantages of both integral backstepping and PID controller algorithms. In a future work, we intend to validate this approach by onboard implementation on a real UAV system.

References

[1] P. Castillo, A. Dzul, and R. Lozano, "Real-time stabilization and tracking of a four-rotor mini rotorcraft," *IEEE Transactions on Control Systems Technology*, vol. 12, no. 4, pp. 510–516, 2004.

[2] H. Romero, S. Salazar, and R. Lozano, "Real-time stabilization of an eight-rotor uav using optical flow," *IEEE Transactions on Robotics*, vol. 25, no. 4, pp. 809–817, 2009.

[3] B. Hérissé, T. Hamel, R. Mahony, and F.-X. Russotto, "A terrain-following control approach for a vtol unmanned aerial vehicle using average optical flow," *Autonomous Robots*, vol. 29, no. 3–4, pp. 381–399, 2010.

[4] F. Sharifi, M. Mirzaei, B. W. Gordon, and Y. Zhang, "Fault tolerant control of a quadrotor uav using sliding mode control," in *Conference on Control and Fault-Tolerant Systems*, 2010, pp. 239–244.

[5] V. G. Adir, A. M. Stoica, and J. F. Whidborne, "Sliding mode control of a 4Y octorotor," *UPB Scientific Bulletin Series D: Mechanical Engineering*, vol. 74, no. 4, pp. 37–52, 2012.

[6] T. K. Roy, H. R. Pota, M. Garratt, and H. Teimoori, "Robust control for longitudinal and lateral dynamics of small scale helicopter," in *31st Chinese Control Conference*, 2012, pp. 2607–2612.

[7] Z. Fang, W. Gao, and L. Zhang, "Robust adaptive integral backstepping control of a 3-dof helicopter," *International Journal of Advanced Robotic Systems*, 2012.

[8] B. Zhu and W. Huo, "Adaptive backstepping control for a miniature autonomous helicopter," in *50th IEEE Conference on Decision and Control*. IEEE, 2011, pp. 5413–5418.

[9] R. Skjetne and T. I. Fossen, "On integral control in backstepping: Analysis of different techniques," in *American Control Conference*, vol. 2, 2004, pp. 1899–1904.

[10] F. Kendoul, "Survey of advances in guidance, navigation, and control of unmanned rotorcraft systems," *Journal of Field Robotics*, vol. 29, no. 2, pp. 315–378, 2012.

[11] L. R. García Carrillo, A. E. Dzul López, R. Lozano, and C. Pégard, *Quad rotorcraft control: Vision-based hovering and navigation*, ser. Advances in Industrial Control Series. Springer London, Limited, 2012.

[12] S. Bouabdallah, "Design and control of quadrotors with application to autonomous flying," Ph.D. dissertation, Ecole Polytechnique Fédérale Lausanne, 2007.

[13] O. Härkegård, "Backstepping and control allocation with applications to flight control," Ph.D. dissertation, Linköping University, 2003.

[14] T. Madani and A. Benallegue, "Control of a quadrotor mini-helicopter via full state backstepping technique," in *45th IEEE Conference on Decision and Control*, 2006, pp. 1515–1520.

[15] L. Mederreg, F. Diaz, and K. N. M'sirdi, "Nonlinear backstepping control with observer design for a 4 rotors helicopter," in *AVCS'04*, I. C. on Advances in Vehicle Control and Safety, Eds., Genova -Italy,, october 2004.

978-1-4799-0275-0/13/$31.00 ©2013 IEEE